Development and Analysis of an RF Film Bulk Acoustic Resonator*

Tang Liang†, Li Junhong, Hao Zhenhong, and Qiao Donghai

(*MEMS Laboratory, Institute of Acoustics, Chinese Academy of Sciences, Beijing* 100190, *China*)

Abstract: A high-Q diaphragm-structure film bulk acoustic resonator (FBAR) with a flat support diaphragm, made of $Si_3N_4/SiO_2/Si_3N_4$ composite films, is proposed. The N/O/N composite diaphragm overcomes the wrinkling in the released support diaphragm caused by the residual stress of a single Si_3N_4 or SiO_2 diaphragm. ZnO piezoelectric film deposited employing a DC reactive magnetron sputtering method is used as the piezoelectric material for the FBAR device. The XRD θ-2θ scan indicates that the ZnO film has the preferred c-axis orientation growth, implying good piezoelectric properties. The S parameter measurement shows that there are three primary resonances in the frequency range from 0.4 to 2.6GHz. The series resonant frequency, parallel resonant frequency, K^2_{eff}, and quality factors of the three resonances are calculated. The third one, with a frequency of about 2.4GHz, has the highest quality factor about 500. Thus, it is expected to be a candidate to form a 2.4GHz low-phase-noise oscillator.

Key words: film bulk acoustic resonator; oscillator; filter; composite diaphragm; ZnO
PACC: 0710C; 7760
CLC number: TN015 **Document code**: A **Article ID**: 0253-4177(2008)11-2226-06

1 Introduction

Recently, the rapid growth of wireless mobile telecommunication systems has led to an increasing demand for high-frequency oscillators, filters, and duplexers operating in the frequency range from 0.5 to 10GHz. Microwave ceramic resonators and surface acoustic wave (SAW) resonators have been conventionally adopted in these applications. However, the former are usually bulky, while the latter suffer high insertion losses and limited power handling capabilities. Moreover, SAW devices can not be integrated at the chip level[1]. Film bulk acoustic resonators (FBARs), which basically consist of a thin layer of piezoelectric material sandwiched between two electrodes, work along the same principle as SAWs— electrical energy is converted to mechanical energy, but unlike SAW devices, the energy is directed into the bulk[2]. Compared to microwave ceramic resonators and SAW resonators, FBAR devices have the advantages of low cost, low insertion losses, high power handling capabilities, high frequency operation, and compatibility with integrated circuit processing[2~4].

The structure of FBAR is largely classified into three types, such as solidly mounted resonators (SMR), air-gap FBARs, and diaphragm-structure FBARs. As for the diaphragm-structure FBAR, Si_3N_4 or SiO_2 is usually used as the supporting material. In our previous work, we found that the residual stress of a single Si_3N_4 or SiO_2 diaphragm often caused wrinkling in the released support diaphragm, which degraded the Q factor dramatically. In this paper, a high-Q diaphragm-structure film bulk acoustic resonator based on ZnO piezoelectric film with a flat support diaphragm, made of $Si_3N_4/SiO_2/Si_3N_4$ composite films, is presented. The performances of ZnO piezoelectric film and FBAR device are analyzed by XRD θ-2θ scan and S parameter measurement, respectively.

2 ZnO piezoelectric film deposition and characterization

It is widely accepted that the (111) plane of Au material has geometric matching to the (002) plane of ZnO piezoelectric film. Thus, sputtered Au film is used as the base layer for ZnO deposition in this study. In order to improve the adherence between the Au film and the Si_3N_4 film, a thin film of Ti was sputtered before the Au film's deposition. ZnO film was deposited using the DC reactive magnetron sputtering method under the condition shown in Table 1. X-ray diffractometer scanning was performed to find properties of ZnO. Figure 1 shows the XRD θ-2θ scan result of ZnO film deposited on Au film. It indicates that the (002) diffraction peak of ZnO film on Au film has high intensity at 34.2° and its full width half maximum (FWHM) value is 0.56°. When ZnO is oriented towards the c-axis perpendicular to the substrate, it has better piezoelectric properties. Figure 1

* Project supported by the National Natural Science Foundation of China (No. 90607012)
† Corresponding author. Email: tangliang@mail.ioa.ac.cn
Received 2 June 2007, revised manuscript received 23 July 2008

Table 1　DC reactive magnetron sputtering condition for ZnO deposition

Target	Zn (99.99%)
Substrate	Au(111)/Ti/Si_3N_4/SiO_2/Si_3N_4/Si
Substrate temperature	280℃
Sputtering voltage	380V
Sputtering pressure	6.7Pa
O_2/Ar	1∶1
Target-substrate distance	100mm
Deposition rate	500nm/h

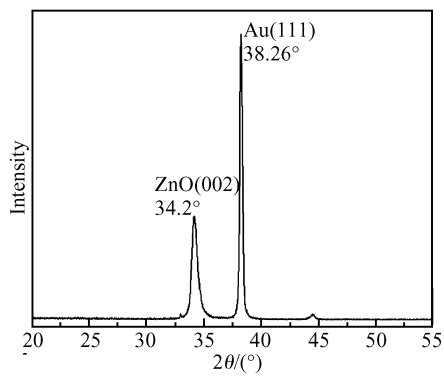

Fig. 1　X-ray diffraction of ZnO piezoelectric film deposited on Au film

confirms that ZnO film has the preferred *c*-axis orientation growth.

3　Film bulk acoustic resonator fabrication

In our previous work, we found that the residual stress of a single Si_3N_4 or SiO_2 diaphragm often caused wrinkling in the released support diaphragm (as shown in Fig. 2(a)), which degraded Q factor dramatically (only about 80). In this work, based on the opposite stress characteristics of Si_3N_4 and SiO_2, a high-Q diaphragm-structure FBAR with a flat support diaphragm, made of Si_3N_4/SiO_2/Si_3N_4 composite films (as shown in Fig. 2(b)), is proposed. Figure 3 shows the fabrication sequence of the FBAR device. First, LPCVD Si_3N_4 films with a thickness of 0.5μm were deposited on both sides of a general 50mm silicon wafer. Then a PECVD SiO_2 film with a thickness of 0.2μm was deposited. After that, LPCVD Si_3N_4 films with a thickness of 0.5μm were deposited on both sides again. Thus Si_3N_4 film, SiO_2 film, and Si_3N_4 film form the N/O/N composite support diaphragm of the FBAR. The etching window for diaphragm structure was fabricated by ICP. Au film and Ti film, with thicknesses of 0.2 and 0.03μm, respectively, were deposited by sputtering and patterned to form the bottom electrode. ZnO piezoelectric film with a thickness of 2μm was deposited using DC reactive magnetron

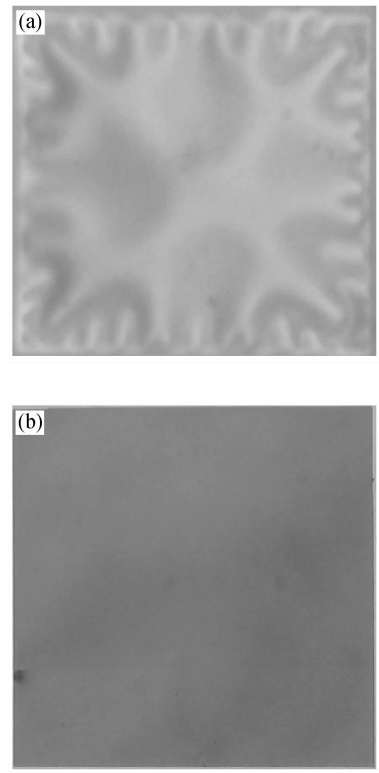

Fig. 2　Morphology of single Si_3N_4 diaphragm with a thickness of 0.5μm (a) and N/O/N composite diaphragm with thicknesses of 0.5μm/0.2μm/0.5μm (b)

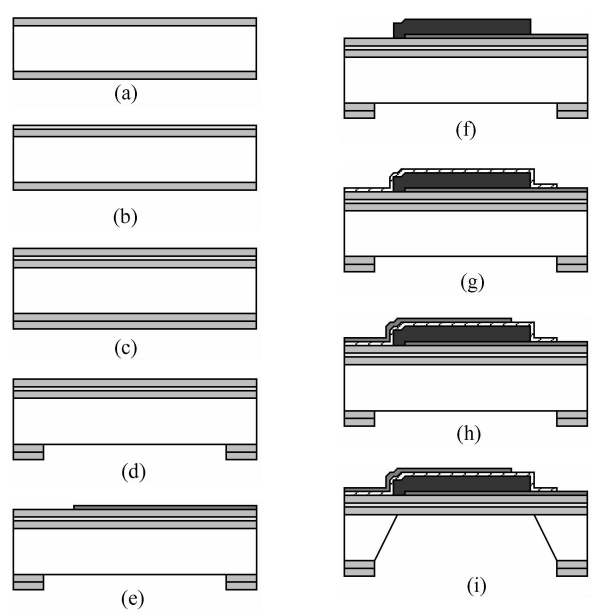

Fig. 3　Fabrication process of the FBAR　(a) LPCVD Si_3N_4 deposition on both sides of a general 50mm silicon wafer; (b) PECVD SiO_2; (c) Another LPCVD Si_3N_4 deposition; (d) Window formation for silicon deep etching; (e) Bottom electrode deposition and patterning; (f) ZnO film deposition and patterning; (g) N/O/N insulated layer deposition and patterning; (h) Top electrode deposition and patterning; (i) Silicon deep etching in KOH solution to form the diaphragm structure

sputtering method and patterned to form the piezoelectric layer. Then another N/O/N composite film with thicknesses of 0.06μm/0.08μm/0.06μm was deposited as an insulated layer and was etched by ICP to open the bottom electrode contact. After that, patterned Au film and Ti film with thicknesses of 0.2 and 0.03μm, respectively, were deposited by the lift-off method to form the top electrode. Finally, the silicon was deeply etched from the backside of the wafer by a 30wt% KOH solution to form the diaphragm structure. The etching temperature was 80℃, and etching rate was about 1.4μm/min. Figure 4 shows the morphology of the fabricated FBAR device. The effective diameter of the device is 200μm and the size is 1.2mm×1.2mm×0.3mm.

4 Results and discussion

To evaluate the performance of the fabricated FBAR device, the S parameter of the FBAR device was measured using an HP8753D network analyzer, and a one-port configuration was adopted, as shown in Fig. 5. The FBAR device is bonded to a test CPW with one pad bonded to the source while the other bonded to the ground.

The ideal one-port resonator with negligibly thin electrodes can be evaluated by a BVD model consisting of a plate capacitance C_0 in parallel with a series R_m-L_m-C_m circuit, shown in Fig. 6 (a). There is a series resonant frequency f_s, set by L_m and C_m, defined by Eq. (1); and a parallel resonant frequency f_p, set by C_0 in series with L_m and C_m, defined by Eq. (2)[5]. In this case, because there is an insulate layer with N/O/N structure between the top electrode and ZnO film, a series capacitor C_s is added at the input. For the inductance and electrical losses induced by the bonding wire, an inductor L_s and a resistor R_s are added in series with C_s. When the operation frequency of the FBAR device is high, the dielectric losses of the piezoelectric material cannot be neglected. Thus, a resistor R_0 is added in parallel with C_0 to evaluate these losses. The modified BVD model to evaluate the performance of FBAR device in our case is shown in Fig. 6 (b).

$$f_s = \frac{1}{2\pi\sqrt{L_m C_m}} \tag{1}$$

$$f_p = \frac{1}{2\pi\sqrt{L_m \dfrac{C_m C_0}{C_m + C_0}}} \tag{2}$$

The resonant characteristics of the FBAR device are shown in Fig. 7. Figure 7 (a) shows the typical plot of the reflection coefficient (S_{11}) and Figure 7 (b) shows the Smith chart. It indicates that there are three primary resonances in the frequency range from

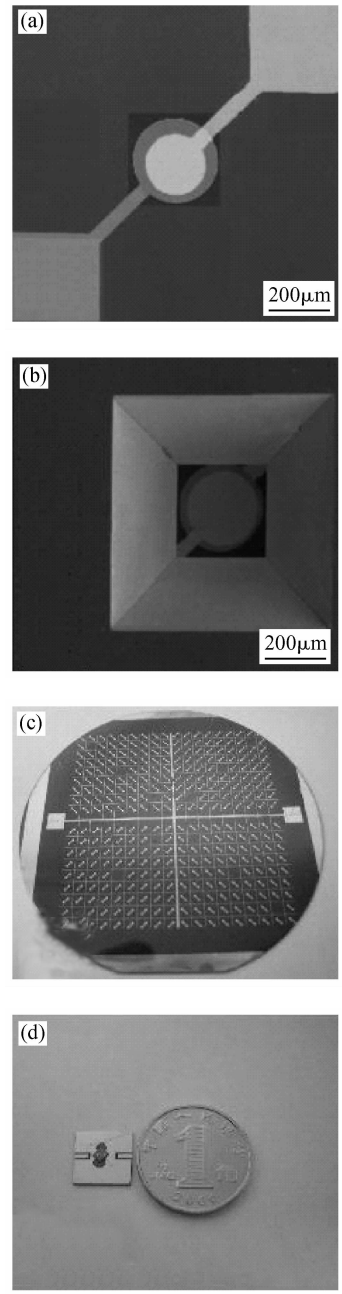

Fig. 4 Morphology of the fabricated FBAR device (a) SEM view from the top; (b) SEM view from the bottom; (c) Array of FBARs in the 50mm wafer; (d) FBAR device bonded to the test CPW

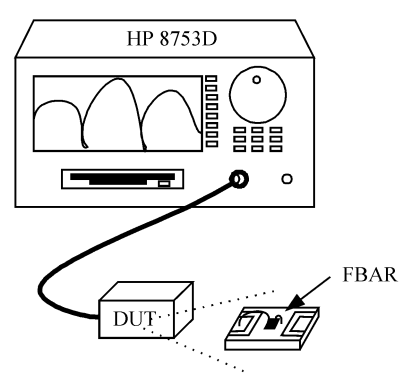

Fig. 5 Sketch map of S parameter measure configuration

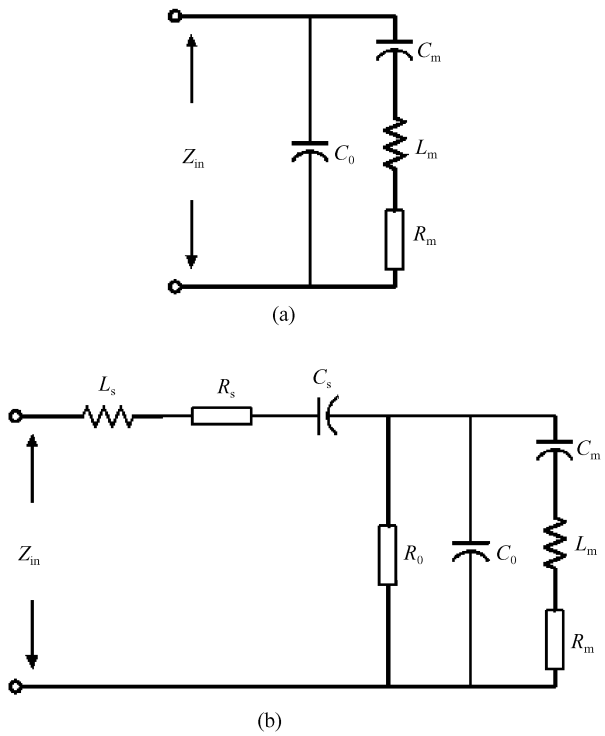

Fig. 6　Equivalent circuits of FBAR device　(a) BVD model; (b) Modified BVD model

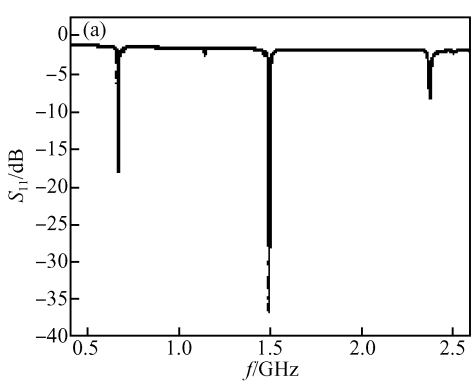

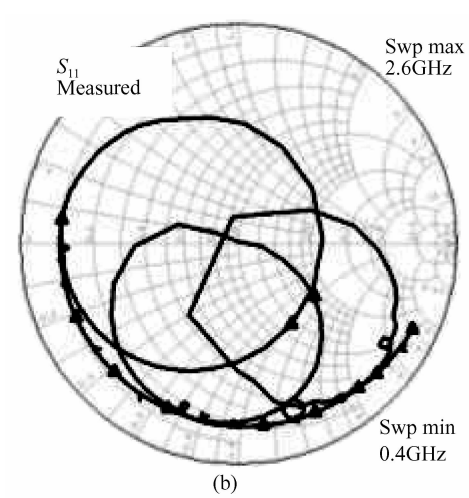

Fig. 7　Measured results of the resonant frequencies　(a) Reflection coefficient (S_{11}); (b) Smith chart

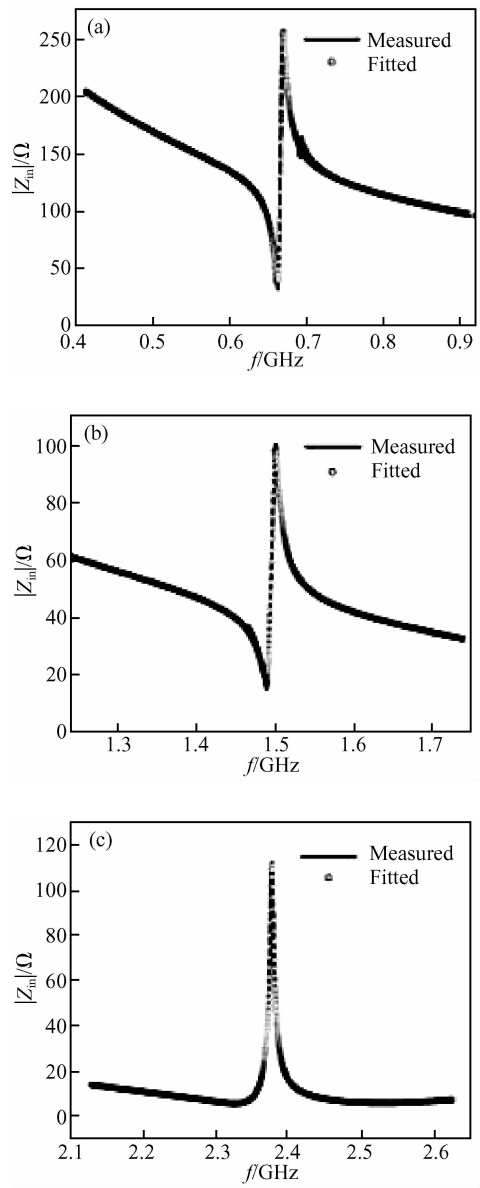

Fig. 8　Measured and fitted results of FBAR device　(a) 1st resonance; (b) 2nd harmonic resonance; (3) 3rd harmonic resonance

0.4 to 2.6GHz. The three resonances, named the 1st resonance, 2nd harmonic resonance, and 3rd harmonic resonance, are fitted using the modified BVD model (shown in Fig. 6 (b)) to extract the parameters of the FBAR device and the parasitic parameters of the bonding wire. Figure 8 shows the measured and fitted curves of the three resonances, and Table 2 shows the extracted parameters.

In this work, the resonant characteristic of the

Table 2　Extracted parameters using modified BVD model

Resonance	L_s /nH	R_s /Ω	C_s /pF	C_0 /pF	R_0 /Ω	L_m /nH	R_m /Ω	C_m /pF
1st	1.052	8.597	4.661	2.737	342.3	755.6	11.66	0.07712
2nd	2.667	3.209	4.426	2.346	384.2	430.0	19.91	0.02654
3rd	2.811	3.847	3.943	2.336	603.7	248.2	6.373	0.01820

Table 3 Characteristics of the fabricated FBAR device

Resonance	f'_s/GHz	f'_p/GHz	$K_{eff}{}^2$	Q_s	Q_p
1st	0.6627	0.6685	2.12%	185	81
2nd	1.4927	1.4982	0.90%	131	102
3rd	2.3714	2.3772	0.60%	500	426

FBAR device is defined by parameters of C_s, C_0, R_0, L_m, C_m and R_m. For the existence of C_s, the equations defining the series and parallel frequencies of FBAR device need to be modified as follows:

$$f'_s = \frac{1}{2\pi}\sqrt{\frac{\frac{1}{C_m}+\frac{1}{C_0+C_s}}{L_m}} \tag{3}$$

$$f'_p = \frac{1}{2\pi\sqrt{L_m\frac{C_mC_0}{C_m+C_0}}} \tag{4}$$

The figure of merit (FOM) of an FBAR device is defined by K^2_{eff} and quality factor. K^2_{eff} is the relative frequency spacing between series resonance frequency and parallel resonance frequency and also a dimensionless measure of electromechanical energy conversion efficiency. The quality factor is a measure of the loss of a resonator[6]. They can be derived using equations as follows[7]:

$$K^2_{eff} = \frac{(\pi/2)(f_s/f_p)}{\tan((\pi/2)(f_s/f_p))} \tag{5}$$

$$Q_{s,p} = \frac{f}{2}\times\frac{\mathrm{d}\angle Z_{in}}{\mathrm{d}f}\Big|_{f_{s,p}} \tag{6}$$

The series resonant frequency f'_s, parallel resonant frequency f'_p, K^2_{eff} and quality factors of the fabricated FBAR devices are calculated using Eqs. (3)~(6), and are summarized in Table 3. The table shows that the quality factor of the 3rd harmonic resonance, with the resonant frequency of about 2.4GHz, is about 500. Thus, it is expected to be a candidate to form a 2.4GHz low-phase-noise RF oscillator. We will fabricate this oscillator in our subsequent work. Furthermore, the reason why the quality factors of the 1st resonance and 2nd harmonic resonance are much lower than the quality factor of the 3rd one will also be revealed in our future work.

5 Conclusion

In this paper, we fabricated a high-Q diaphragm-structure FBAR with a flat support diaphragm, which is made of $Si_3N_4/SiO_2/Si_3N_4$ composite films. The N/O/N composite diaphragm overcomes the wrinkling in the released support diaphragm caused by the residual stress of a single Si_3N_4 or SiO_2 diaphragm. The FBAR device is based on ZnO piezoelectric film. We deposited the ZnO piezoelectric film employing a DC reactive magnetron sputtering method, and the XRD θ-2θ scan indicates that the ZnO film has the preferred c-axis orientation growth. The S parameter measurement shows that there are three primary resonances in the frequency range from 0.4 to 2.6GHz, namely the 1st resonance, 2nd harmonic resonance, and 3rd harmonic resonance. The series resonant frequency, parallel resonant frequency, K^2_{eff}, and quality factors of the three resonances are calculated. The 3rd one among the three resonances, with the resonant frequency of about 2.4GHz, has the highest quality factor about 500. It is expected to be a candidate to form a 2.4GHz low-phase-noise oscillator. In our future work, we will fabricate a 2.4GHz oscillator based on this FBAR device. Furthermore, the reason why the quality factors of the 1st resonance and 2nd harmonic resonance are much lower than the quality factor of the 3rd one will also be revealed.

Acknowledgements The authors would like to thank Mr. Wang Chenghao, who is an academician of the Chinese Academy of Sciences, for his advice in designing the FBAR device.

References

[1] Huang C L, Tay K W, Wu L. Aluminum nitride films deposited under various sputtering parameters on molybdenum electrodes. Solid-State Electron, 2005, 49(2): 219

[2] Ruby R C, Bradley P, Oshmyansky Y, et al. Thin film bulk wave acoustic resonators (FBAR) for wireless applications. IEEE Ultrasonics Symposium, 2001, 1: 813

[3] Larson J D, Ruby R C, Bradley P, et al. Power handling and temperature coefficient studies in FBAR duplexers for the 1900MHz PCS band. IEEE Ultrasonics Symposium, 2000, 1: 869

[4] Ruby R, Bradley P, Larson J, et al. Ultra-miniature high-Q filters and duplexers using FBAR technology. IEEE International Solid-State Circuits Conference, 2001: 120

[5] Larson J D, Ruby R, Bradley P, et al. A BAW antenna duplexer for the 1900MHz PCS band. IEEE Ultrasonics Symposium, 1999, 2: 887

[6] Kang Y R, Kang S C, Paek K K, et al. Air-gap type film bulk acoustic resonator using flexible thin substrate. Sensors and Actuators A, 2005, 117(1): 62

[7] Lakin K M, Kline G R, McCarron K T. High-Q microwave acoustic resonators and filters. IEEE Trans Microw Theory Tech, 1993, 41(12): 2139

射频薄膜体声波谐振器的研制和分析*

汤　亮†　李俊红　郝震宏　乔东海

（中国科学院声学研究所 声学微机电实验室，北京　100190）

摘要：研制了一种采用氮化硅/二氧化硅/氮化硅复合膜作为支持薄膜的高 Q 薄膜体声波谐振器.当采用单层氮化硅膜或二氧化硅膜作为谐振器的支持薄膜时，由于残余应力的作用，释放完的薄膜往往会出现褶皱的现象，极大地降低了薄膜体声波谐振器的 Q 值；上述复合膜结构有效地解决了这个问题.采用直流磁控溅射法制备了氧化锌压电薄膜，X 射线衍射结果表明制备的氧化锌薄膜具有很好的 c 轴择优取向，意味着氧化锌薄膜具有较好的压电性.S 参数测试结果表明该薄膜体声波谐振器在 0.4～2.6GHz 的频率范围内具有 3 个明显的谐振模式，计算了这些谐振模式的串联谐振频率、并联谐振频率、有效机电耦合系数和 Q 值.在这 3 个模式中，第 3 个谐波模式的工作频率约为 2.4GHz，具有最高的 Q 值（约为 500），可用来制备 2.4GHz 的低相噪射频振荡源.

关键词：薄膜体声波谐振器；振荡器；滤波器；复合膜；氧化锌

PACC：0710C；7760

中图分类号：TN015　　**文献标识码**：A　　**文章编号**：0253-4177(2008)11-2226-06

* 国家自然科学基金资助项目（批准号：90607012）

† 通信作者.Email：tangliang@mail.ioa.ac.cn

2008-06-02 收到，2008-07-23 定稿